Analyzing Topology Dynamics in Ad Hoc Networks Using A Smooth Mobility Model

Ming Zhao Wenye Wang

Department of Electrical and Computer Engineering
North Carolina State University
Raleigh, North Carolina 27695–7911
Email: {mzhao2, wwang}@ncsu.edu

***Abstract*— Understanding the impacts of node mobility on topology dynamics is essential to design a mobility resilient ad hoc network. Current research showed that mobility models can heavily affect the study of network topology due to different mobility patterns. In this paper, we analyze topology dynamics based on the *smooth* model [1], because it generates smooth nodal movements, has no speed decay problem, and maintains a uniform spatial node distribution. Specifically, we study two topology metrics: *expected link lifetime* and *expected link change rate* by using a distance transition probability matrix P, in which an element represents the distance change between two neighboring nodes. By this means, we predict the existence of a link based on the present distance between a pair of nodes and their relative speed. The analytical results of topology dynamics are validated by extensive simulations. In addition, by combing graph theory and queuing theory, we apply the topology metrics *expected link lifetime* and *expected link change rate* to formulate the upper bound connectivity of a mobile ad hoc network.**

I. Introduction

In mobile ad hoc networks (MANETs), node mobility induces the network topology to change randomly and rapidly at unpredictable times. Hence, the network topology is vulnerable to frequent link failure and network partitioning, which could incur substantial routing overhead, excessive transmission delay and packet loss among mobile nodes. Hence, in order to design a mobility resilient MANET, an intuitive solution is to enlarge the transmission range of the mobile wireless devices for reducing the network topology change rate. However, by this way, the mobile nodes would suffer more radio interference, channel contention, and energy consumption, which may seriously degrade the utilization of the network resources. Therefore, to achieve the desired network performance, it is necessary to investigate the property of node mobility and its effect on topology dynamics of MANETs.

In a MANET, routing protocols are used to deliver data between mobile nodes, depending on the link status between any pair of mobile nodes. The dynamics of links directly dominates the network topology change rate and the network performance. Hence, we investigate topology dynamics by analyzing two key topology metrics: *expected link lifetime* and *expected link change rate* in this paper. The study of link properties is based on mobility models, which specify node moving behaviors in a MANET [2]. Random mobility models [3], such as random waypoint (RWP) model [4], are the most widely used mobility models in the current research of MANETs. Because nodal movements in random mobility models are total randomness, the unrealistic moving behaviors, such as sudden speed change and sharp turn, may invalidate the analytical and simulation results of topology metrics [3]. Moreover, Yoon et al. showed that the average node speed of the RWP model decreases over time [5]. Hence, the unexpected lower mobility level will increase the expected link lifetime in the RWP model. Furthermore, Bettstetter et al. found that the RWP model yields non-uniform spatial node distribution, with the maximum node density in the center of simulation region [6]. This non-uniform spatial node distribution could invalidate many analytical and simulation results that are based on the assumption of uniform spatial node distribution of a MAENT. Because of the limitations of the random mobility models, it is highly desirable to use a new mobility model for analyzing topology dynamics.

In this paper, we analyze topology dynamics based on the *smooth* mobility model proposed in [1]. The smooth movements specified in the model abide by the physical law of real-life moving objects, so that mobile nodes can smoothly change their velocities within a movement, which avoids the abrupt moving behaviors happening in the random mobility models. In addition, the smooth model generates stable node speed and maintains a uniform spatial node distribution. We assume that all mobile nodes of a MANET have the same transmission range R. Hence, at an arbitrary time, by comparing the distance of a pair of nodes with their common transmission range R, we can determine the existence of their link. Further, we can predict the link duration and link change rate based on the present distance between a pair of nodes and their relative speed. Specifically, we analyze *expected link lifetime* and *expected link change rate* of MANETs by using a distance transition probability matrix $\mathbf{P}$. Based on these analytical results, we investigate how to utilize the topology metrics to estimate network connectivity. Our study on topology dynamics can help people design mobility resilient routing protocols and optimize topology control schemes of MANETs.

The remainder of the paper is organized as follows. Section II characterizes the relative movement of two nodes under the smooth model and describes all preliminaries necessary for analyzing topology dynamics. In Section III, we derive theoretical expressions of topology metrics and validate them by simulations. Then, we utilize topology metrics to evaluate MAENT connectivity. Section IV concludes this paper.

II. Mobility Characterization in MANETs

We study topology dynamics by analyzing MANET link properties, which are characterized by the relative movement and separated distance of two neighboring nodes. Hence, in this section, we first specify the mobility pattern of the smooth model, upon which we propose a relative movement trajectory model of two nodes for analyzing link properties. Next, we develop a distance transition probability matrix $\mathbf{P}$ based on the distribution of the relative speed in the smooth model. Each element of the matrix $\mathbf{P}$ represents a single step transition probability of distance change between two nodes. By applying the matrix $\mathbf{P}$, we can predict the link lifetime and link change rate based on the present distance and the relative speed between two neighboring nodes.

A. Smooth Mobility Model

To follow the physical law of a smooth motion, each movement in the smooth model contains three consecutive moving phases: Speed Up (α–phase), Middle Smooth (β–phase), and Slow Down (γ–phase). Each movement is quantized into random $\mathcal{K}$ equidistant *time steps*, where $\mathcal{K} = \alpha + \beta + \gamma$ and $\mathcal{K} \in \mathbb{Z}$. The time interval between two consecutive time steps is Δt (sec). For each movement, a node will select a target direction ϕ_α, and a target speed v_α, which is the stable speed of the movement. Specifically, in α–phase, it uniformly accelerates its speed to v_α for α time steps along the direction ϕ_α. For each time step in β–phase, where the node moves at the stable velocity of the movement, the node speed and direction gently fluctuate around v_α and ϕ_α, respectively. In γ–phase, the node uniformly decelerates its speed to 0 for γ time steps along a selected direction ϕ_γ. After the movement, the node pauses at a random time T_p, which is considered as the pause phase of the smooth model [1].

Since the node movement abides by the physical law of a smooth motion, the smooth model is more realistic than random mobility models. Furthermore, as proved in [1], the smooth model has no speed decay problem [5] and maintains uniform nodal spatial distribution. These nice properties are crucial to analyze topology dynamics of MANETs.

B. Relative Movement Trajectory Model

A valid analysis of topology dynamics should be based on a realistic moving scenario of MANETs. In reality, the relative velocity of two mobile nodes changes during their link connection, due to their speed acceleration/deceleration and possible direction change within each movement. Based on this observation, we provide a relative movement trajectory model upon which Fig. 1 illustrates a sample relative movement trajectory between a node pair (u, w) during their link connection. As the reference node, node u lies in the original point of Cartesian coordinate system XY. We assume that the link between the node pair (u, w) forms immediately after

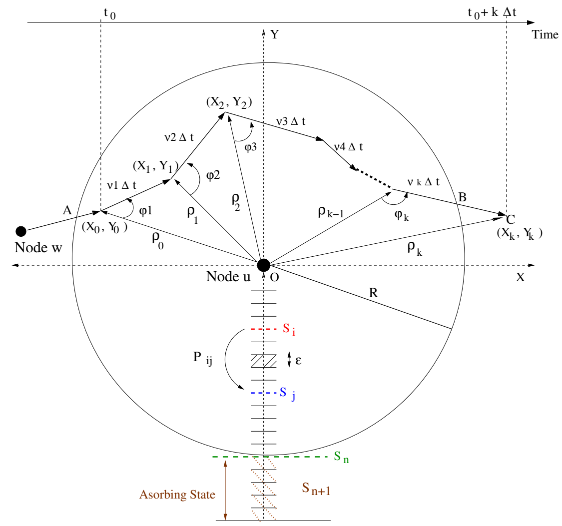

Fig. 1. A sample of a relative movement trajectory between a node pair (u, w) during their link connection.

the time step when node w transits the border of node u's transmission zone. Given the example shown in Fig. 1, the link forms at time t_0. Then, it takes k time steps for node w to first move outside the transmission zone from position B. For the sake of simplicity, the time step Δt is normalized to 1 second in this paper. Hence, the link lifetime T_{link} of the node pair (u, w) is $T_{link} = k$ seconds, where $k >> 1$. We denote $\overrightarrow{v_i}$ as the relative speed and $\overrightarrow{\rho_i}$ as the vector of the ending position of i^{th} time step of node w according to the XY coordinate. Correspondingly, ρ_i is the magnitude of $\overrightarrow{\rho_i}$, where $\rho_i = \sqrt{{X_i}^2 + {Y_i}^2}$. We assume that both the relative speed $\overrightarrow{v_i}$ and the angle ψ_i are i.i.d. random variables (RVs).

C. Distance Transition Probability Matrix $\mathbf{P}$

As shown in Fig. 1, once node w moves into node u's transmission zone, the link status is determined by the distance between two nodes at every Δt, i.e., every time step. Hence, we develop a distance transition probability matrix $\mathbf{P}$ to analyze link properties of MANETs.

In Fig. 1, the transmission range R of node u is quantized into n equidistant length intervals with a width of ε meters. Hence, $R = n \cdot \varepsilon$. Each length interval is corresponding to a state representing the distance between node u and node w. For example, the range of distance indexed by state S_i is over $[(i-1)\varepsilon, i\varepsilon]$. Because of the node mobility, the distance between node pair (u, w) may vary after each time step. Hence, We denote $\mathbf{P}$ as the distance transition probability matrix, and P_{ij} as the probability of state transition from S_i to S_j after a single time step. From Fig. 1, the link expires when the event of $\rho_k > R$ first happens. Accordingly, we let state S_{n+1} represent all the locations which lie outside node u's transmission zone. Since link connection breaks as long as node w reaches state S_{n+1}, we define state S_{n+1} as the *absorbing state* of $\mathbf{P}$.

As the target speed v_α represents the stable speed of a movement in the smooth model, P_{ij} is characterized by the target speed v_α of mobile nodes. Moreover, because the node speed at each time step of β–phase fluctuates around v_α based on the Gauss-Markov mobility pattern [1], the relative speed range of node w according to v_α is over $[0, 2(v_\alpha + \delta_v)]$, where the empirical value of δ_v is 2 m/sec. For instance, being at state S_i, the possible states for node w after one time step movement are in the range $[\max(1, i-r), \min(i+r, n+1)]$, where $r = \lceil 2(v_\alpha + \delta_v)/\varepsilon \rceil$. Based on this argument, Fig. 2 demonstrates the distance transition probability matrix $\mathbf{P}$, in which all positive elements, i.e., ($P_{ij} > 0, \;\; 1 \le i, j \le n+1$), are within the shadow area.

The distance transition probability matrix $\mathbf{P}$ plays an essential role for deriving topology metrics. Next, following the similar strategy described in [7], we provide a way for calculating P_{ij} in terms of target speed v_α.

1) Single-Step Transition Probability P_{ij} : From Fig. 1, at the m^{th} step, $\overrightarrow{\rho}_m = \overrightarrow{\rho}_{m-1} + \overrightarrow{v}_m$. Hence, we have

$$\rho_m = \sqrt{\rho_{m-1}^2 + {v_m}^2 - 2\rho_{m-1} v_m \cos\psi_m}, \tag{1}$$

where ψ_m is uniformly distributed from $[0, \pi)$. From (1), ψ_m can be represented as:

$$\psi_m = \arccos \frac{{\rho_{m-1}}^2 + {v_m}^2 - {\rho_m}^2}{2\rho_{m-1} v_m}. \tag{2}$$

Given the relationship between ρ_{m-1} and ρ_m, the single-step transition probability P_{ij} can be derived as:

$$\begin{aligned} & P_{ij} = Prob\{\rho_m \in S_j \mid \rho_{m-1} \in S_i\} \\ = \; & \frac{\int_{(j-1)\varepsilon}^{j\varepsilon} \int_{(i-1)\varepsilon}^{i\varepsilon} f_{\rho_m|\rho_{m-1}}(\rho_m|\rho_{m-1}) f(\rho_{m-1}) d\rho_{m-1} d\rho_m}{\int_{(i-1)\varepsilon}^{i\varepsilon} f(\rho_{m-1}) d\rho_{m-1}}. \end{aligned} \tag{3}$$

Upon (3), it is necessary to find the conditional distribution $f_{\rho_m|\rho_{m-1}}(\rho_m \mid \rho_{m-1})$ to solve P_{ij}. Here, v_m and ψ_m are independent RVs. From (2), ψ_m is a strictly monotonous function of ρ_m. Hence, given a specific target speed v_α for mobile nodes in the smooth model, we have

$$\begin{aligned} & f_{\rho_m|\rho_{m-1}}(\rho_m \mid \rho_{m-1}) \\ = \; & \int_0^{2(v_\alpha+\delta_v)} f_{\rho_m|\rho_{m-1}, v_m}(\rho_m \mid \rho_{m-1}, v_m) \cdot f_V(v_m) dv_m \\ = \; & \int_0^{2(v_\alpha+\delta_v)} f_{\psi_m}(\psi) \cdot \left|\frac{\partial \psi_m}{\partial \rho_m}\right| \cdot f_V(v_m) dv_m \\ = \; & \int_0^{2(v_\alpha+\delta_v)} \frac{\frac{2}{\pi}\rho_m \cdot f_V(v_m) dv_m}{[4\rho_{m-1}^2 {v_m}^2 - ({\rho_{m-1}}^2 + {v_m}^2 - {\rho_m}^2)^2]^{1/2}}. \end{aligned} \tag{4}$$

where $f_V(v)$ is the PDF of the relative speed. From (3) and (4), $f_V(v)$ is a key element for calculating the value of P_{ij}. However, a node speed for an arbitrary time step may stay in one of the four phases of the smooth model. Furthermore, a node speed varies in every time step within a moving phase. Hence, how to derive the relative speed distribution in the smooth model is very challenging. Next, we derive the distribution of $f_V(v)$ through the statistical analysis of simulation data of the relative speed in the smooth model.

2) Relative Speed Distribution $f_V(v)$: As shown in Fig. 1, both the relative speed $\overrightarrow{v_i}$ and the angle ψ_i of node w are i.i.d. RVs. Then, according to the analytical result in [8], both X_k and Y_k can be efficiently approximated by Gaussian random

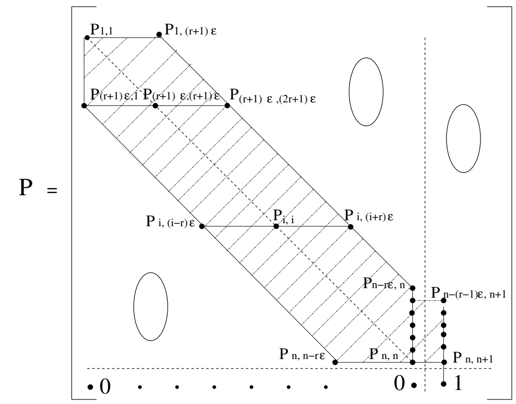

Fig. 2. Distance transition probability matrix $\mathbf{P}$.

distribution when $k >> 1$. Given Fig. 1, the magnitude of k^{th} step relative speed v_k is represented as:

$$v_k = \sqrt{(X_k - X_{k-1})^2 + (Y_k - Y_{k-1})^2}, \tag{5}$$

where both RV $X_k - X_{k-1}$ and $Y_k - Y_{k-1}$ can be effectively approximated by an identical Gaussian distribution with zero mean. Furthermore, from the theoretical result shown on pp. 140 in [9]: If the RVs X and Y are normal, independent with zero mean and equal variance, then the RV $Z = \sqrt{X^2 + Y^2}$ has a *Rayleigh density* as follows:

$$f_Z(z) = \frac{z}{a^2}\, e^{\frac{-z^2}{2a^2}} U(z) \quad \text{and} \quad E\{z\} = a\sqrt{\pi/2}. \tag{6}$$

Therefore, when k is large, we found that the distribution of relative speed in (5) can be approximated by *Rayleigh* distribution. As the target speed v_α characterizes the stable speed of a movement in the smooth model, we set the expected relative speed $E\{v\}$ as v_α. Corresponding to (6), $E\{v\} = v_\alpha = a\sqrt{\pi/2}$, then the PDF of relative speed is:

$$f_V(v) = \frac{v}{(v_\alpha\sqrt{\frac{2}{\pi}})^2}\; e^{\frac{-v^2}{2(v_\alpha\sqrt{\frac{2}{\pi}})^2}} = \frac{\pi v}{2{v_\alpha}^2}\; e^{\frac{-\pi v^2}{4{v_\alpha}^2}}. \tag{7}$$

To validate the expression in (7), we obtain the experimental relative speed distribution $f_V(v)$ between two neighboring nodes by simulations. The smooth model is simulated through ns-2 simulator. In detail, 50 mobile nodes, with the same transmission range $R = 250$ m, move in an area of $1401 \times 1401\ m^2$ for a period of 500 seconds, such that the node density is $\sigma = 5/\pi R^2$. On purpose to investigate the distribution $f_V(v)$ under different levels of node speed, we respectively set the target speed v_α to $2, 5, 10, 15, 20$ m/sec. In each scenario, $E\{\alpha\} = E\{\beta\} = E\{\gamma\}$, and pause time $T_p = 0$. Fig. 3 illustrates the PDF of relative speed resulted from both simulation and the theoretical expression in (7) versus different values of v_α. We observed that the proposed Rayleigh distribution with metric v_α matches very well with the distribution of relative speed obtained by simulation, especially when v_α is small. This is because a smaller v_α implies a larger number of k relative steps, such that a better Gaussian approximation of X_k/Y_k, in turn, a better Rayleigh distribution approximation of the relative speed in the smooth model can be achieved. Therefore, $f_{\rho_m|\rho_{m-1}}(\rho_m \mid \rho_{m-1})$ can be calculated by substituting $f_V(v)$ obtained from (7) into (4).

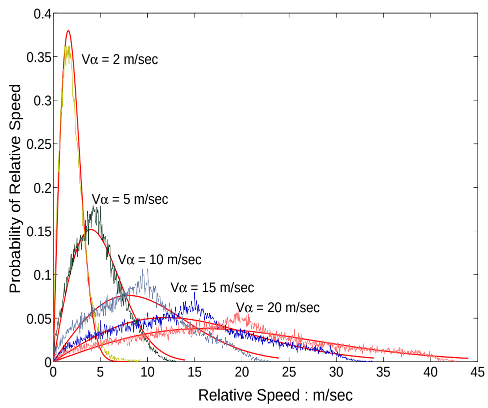

Fig. 3. Comparison of the experimental relative speed distribution with the Rayleigh distribution approximation.

Upon the arguments of P_{ij} in [7], if the number of states in the matrix $\mathbf{P}$ is larger enough, i.e., ε is sufficiently small, we can effectively use the middle points $(i-\frac{1}{2})\cdot\varepsilon$ and $(j-\frac{1}{2})\cdot\varepsilon$ to represent the value of ρ_{m-1} and ρ_m, respectively. Then, P_{ij} derived in (3) can be effectively approximated as:

$$P_{ij} \approx \varepsilon \cdot f_{\rho_m|\rho_{m-1}}[(j-\frac{1}{2})\cdot\varepsilon \mid (i-\frac{1}{2})\cdot\varepsilon)]. \quad (8)$$

By far, we obtained all the necessary knowledge for constructing the matrix $\mathbf{P}$ with respect to different target speeds v_α of the smooth model. By using the matrix $\mathbf{P}$, we analyze topology dynamics of MANETs in the next section.

III. Analysis of Topology Dynamics

The *expected link lifetime* $\overline{T}_{link}$ and *expected link change rate* η_l are two fundamental topology metrics, which can effectively indicate the dynamic degree of network topology in the presence of the node mobility. In this section, we first analyze these topology metrics by using the distance transition probability matrix $\mathbf{P}$ and validate the theoretical results by simulation. Then, we apply $\overline{T}_{link}$ and η_l to formulate the upper bound connectivity of a MANET.

A. Expected Link Lifetime

In order to derive the expected link lifetime, we first analyze the CDF and PMF of link lifetime as follows.

Let $\pi^{(0)}$ denote the probability of the initial state that node w lies when the link is setting up. Thus, $\pi^{(0)}$ is a row vector with $n+1$ elements. Correspondingly, we denote $\pi_i(m)$ as the probability that node w lies in state S_i after the m^{th} step. Hence, $\pi^{(m)} = \Big(\pi_1(m), \cdots, \pi_i(m), \cdots, \pi_{n+1}(m)\Big)$. For easy representation, we denote the distance transition probability matrix $\mathbf{P}$ as $\mathbf{P} = [P_1, \cdots, P_i, \cdots, P_{n+1}]$ and P_i is the i^{th} column vector of $\mathbf{P}$. Upon the law of matrix multiplication, we have the equation $\pi^{(0)} \cdot \mathbf{P} = [\pi^{(0)}P_1, \cdots, \pi^{(0)}P_i, \cdots, \pi^{(0)}P_{n+1}]$. As S_{n+1} is the absorbing state, $\pi^{(0)}P_{n+1}$ represents the probability that node w moves outside the transmission zone after 1st time step from its initial position. Hence, given the knowledge of $\pi^{(0)}$ and the distance transition probability matrix $\mathbf{P}$, we can derive the CDF of link lifetime distribution as follows:

$$Prob\{T_{link} \le m\} = \pi_{n+1}(m) = \pi^{(0)}\mathbf{P}^m(n+1), \quad (9)$$

where $\pi^{(0)}\mathbf{P}^m(n+1)$ is the probability of the $(n+1)^{th}$ element of the row vector $\pi^{(0)}\mathbf{P}^m$. Following (9), the PMF of link lifetime distribution is derived as:

$$\begin{aligned} & Prob\{T_{link} = m\} \\ = \; & Prob\{T_{link} \le m\} - Prob\{T_{link} \le m-1\} \\ = \; & \pi^{(0)}\mathbf{P}^m(n+1) - \pi^{(0)}\mathbf{P}^{m-1}(n+1). \end{aligned} \quad (10)$$

From (10), the expected link lifetime $\overline{T}_{link}$ as a function of m is represented as:

$$\overline{T}_{link} = \sum_{m=1}^{\infty} m[\pi^{(0)}\mathbf{P}^m(n+1) - \pi^{(0)}\mathbf{P}^{m-1}(n+1)]. \quad (11)$$

According to Fig. 1, the initial state distribution $\pi^{(0)}$ relies on the initial position (X_0, Y_0) of node w. Following the same argument in Section II-C, when node w transits into node u's transmission zone, there is maximum r possible states that node w can reach within one time step, where $r = \lceil 2(v_\alpha + \delta_v)/\varepsilon \rceil$. Hence, the possible states that the initial position (X_0, Y_0) of node w can stay are from S_{n-r+1} to S_n. To obtain $\pi^{(0)}$, we assume that node w lies in these r states with an equal probability as $\frac{1}{r}$. Hence, given $\pi^{(0)}$ and $\mathbf{P}$, the expected link lifetime $\overline{T}_{link}$ is obtained from (11). To validate the analytical results of $\overline{T}_{link}$ derived in (11), Fig. 4 demonstrates both simulation results and theoretical calculation of expected link lifetime with respect to different node target speed $v_\alpha = 2, 5, 10, 15, 20$ m/s, respectively. We can see that the theoretical results match with the simulation data. As the node speed increases, $\overline{T}_{link}$ decreases dramatically when v_α is within the range $[2, 10]$ m/sec, and the downtrend of $\overline{T}_{link}$ slows down when $v_\alpha > 10$ m/sec. As an illustration, $\overline{T}_{link}$ lasts 4 times longer for nodes moving at the target speed of 2 m/sec than that at the target speed of 20 m/sec.

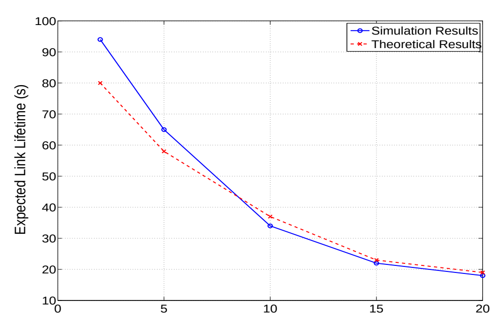

Fig. 4. Comparison of expected link lifetime between simulation results and theoretical results according to $v_\alpha = 2, 5, 10, 15, 20$ m/s, respectively.

B. Expected Link Change Rate

Here, we analyze the expected link change rate, which is defined as the expected number of link changes per second observed by a single node. From the viewpoint of node u, assume that the total number of new link arrivals, i.e., the total number of new mobile nodes moving into its transmission zone, during time interval $[0, t]$ is $N_a(t)$. And the total number of link breakages for the node u during time interval $[0, t]$ is $N_b(t)$. Then, we denote the *expected new link arrival rate* λ as $\lambda = \lim_{t\to\infty} \frac{N_a(t)}{t}$ and the *expected new link breakage rate* μ_b as $\mu_b = \lim_{t\to\infty} \frac{N_b(t)}{t}$, respectively. In [10], Samar et al. showed that the expected new link arrival rate λ is equal to the expected link breakage rate μ_b in a MANET. Let η_l denote the *expected link change rate*. Then, we have

$$\eta_l = \lambda + \mu_b = 2\lambda. \tag{12}$$

From (12), the expected link change rate η_l is two times as large as the expected new link arrival rate λ. According to Fig. 1, λ is equivalent to the expected number of new nodes entering node u's transmission zone at every time step. As shown in Fig. 5, we extend the total number of states to $n+r$, where $r = \lceil 2(v_\alpha + \delta_v)/\varepsilon \rceil$. Hence, within one time step, the furthest state a node can reach is r states away from its current state. Therefore, a node could enter node u's transmission zone at the next time step, only if it is currently lying in one of the states among $\{S_{n+1}, S_{n+2}, ..., S_{n+r}\}$. Let $P_{la}(n+i)$ denote the probability that a node in state S_{n+i} will move into the transmission zone of node u within the next time step. Then, $P_{la}(n+i)$ is represented as:

$$P_{la}(n+i) = \sum_{j=n+i-r}^{n} P_{n+i,j} \quad , \quad 1 \le i \le r, \tag{13}$$

where $P_{n+i,j}$ can be obtained from (4) and (8), respectively. Furthermore, according to the state S_{n+i}, we denote the region $\mathbf{D}_{n+i}$ as the the set of all positions whose distances to the reference node u are in the range $[(n+i-1)\varepsilon, (n+i)\varepsilon]$. As shown in Fig. 5, the area of $\mathbf{D}_{n+i}$ is the area of a circular ring, which has the outer radius $(n+i)\varepsilon$ and the inner radius $(n+i-1)\varepsilon$, respectively. Hence, we have $S(\mathbf{D}_{n+i}) = \pi\varepsilon^2[(n+i)^2 - (n+i-1)^2] = \pi\varepsilon^2(2i+2n-1)$. Let σ denote the node density of a MANET, which maintains a uniform distribution of node location. Then, $\sigma \cdot S(\mathbf{D}_{n+i})$ is the average number of nodes lie inside the area $\mathbf{D}_{n+i}$. Therefore, by combing all possible regions $\mathbf{D}_{n+i}$, $1 \le i \le r$, λ is derived as:

$$\begin{aligned} \lambda &= \sum_{i=1}^{r} P_{la}(n+i) \cdot \sigma \cdot S(\mathbf{D}_{n+i}) \\ &= \sigma\pi\varepsilon^2 \sum_{i=1}^{r} \sum_{j=n+i-r}^{n} P_{n+i,j} \cdot (2i+2n-1). \end{aligned} \tag{14}$$

To validate the analytical results for η_l and λ in (12) and (14), respectively. We compare the theoretical results to the simulation results according to the node target speed v_α in Fig.6. As can be observed, the analytical results are verified by the the simulations results. Upon Fig. 6, we also found that given a fixed transmission change R, both η_l and λ grow linearly with the increase of the node speed, especially when $v_\alpha \ge 5$ m/sec. For instance, when $R = 250$ m, the slope of the expected link change rate versus the node speed is 0.28. Based on this relation between η_l and v_α, we can directly estimate the change rate of network topology with different node speed level in the smooth model.

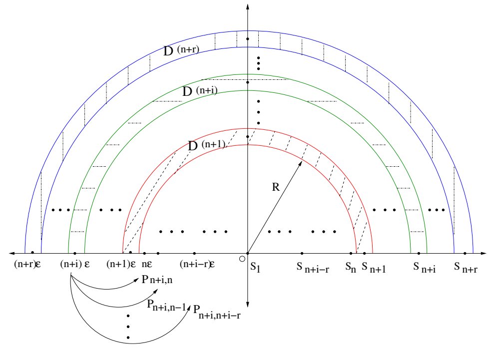

Fig. 5. Derivation of expected new link arrival rate λ.

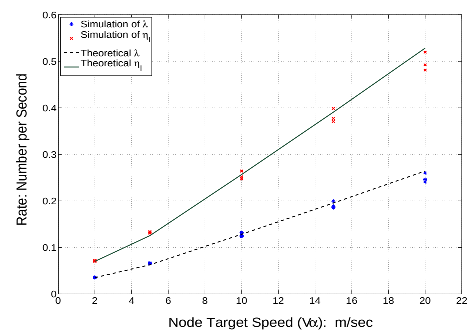

Fig. 6. Comparison of expected new link arrival rate λ and expected link change rate η_l between simulation results and theoretical results, according to different node target speeds v_α, where $\sigma = 5/\pi R^2$, $R = 250$m.

C. Discussion on Network Connectivity

Here, we utilize the knowledge of expected link lifetime $\overline{T}_{link}$ and expected link change rate η_l to investigate their relationship with the average node degree for estimating the network connectivity. Based on the definition of *graph connectivity* in [11], the *connectivity* of the network $G(t)$ denoted by $\kappa(G(t))$ is defined as: the maximum value of k, for which a connected network $G(t)$ is k-connected at time t. Let $d_{G(t)}(u)$ denote the *degree* of node u in $G(t)$, which is the number of edges of $G(t)$ incident with node u. Let $\delta(G(t))$ and $E\{d_{G(t)}\}$ be the minimum degree and average degree of $G(t)$, respectively. From the graph theory, $\kappa(G(t))$, $\delta(G(t))$ and $E\{d_{G(t)}\}$ satisfy the inequality [11]:

$$\kappa(G(t)) \le \delta(G(t)) \le E\{d_{G(t)}\}. \tag{15}$$

From (15), $E\{d_{G(t)}\}$ is the upper bound of the connectivity of a MANET $G(t)$. Thus, $E\{d_{G(t)}\}$ is a key parameter for evaluating network connectivity. Next, we study the property of MANET connectivity based on $E\{d_{G(t)}\}$ as follows.

In a MANET $G(t)$, we consider that each node is associated with a queuing system. As shown in Fig. 1, for the queuing system of node u, the event that node w is moving into its transmission zone, denoted by $\mathbf{A}_u$, is referred to a new arrival coming into the system. And the event of node w moving outside the transmission zone $\mathbf{A}_u$ is regarded as a departure to the system. According to the Little's law of a queuing system [9]: the average number of customers L in the system is equal to the average arrival rate Λ of customer to the system multiplied by the average system time W per customer, that is, $L = \Lambda W$. Because the link between the node pair (u, w) immediately forms once node w transits into node u's transmission zone, there is no waiting time for node w in the queuing system of node u. Thus, the system time node w spends is from the instant of its arrival into $\mathbf{A}_u$ to the instant of its departure from $\mathbf{A}_u$, which is equivalent to the link lifetime of the node pair (u, w), i.e., $W = \overline{T}_{link}$. And the average customer arrival rate Λ to the queuing system of node u is equivalent to the expected new link arrival rate λ of node u, i.e., $\Lambda = \lambda$. Consequently, the average number of system customers of a mobile node is equivalent to the average number of neighbors of that node, that is, $L = E\{d_{G(t)}\}$. Hence, with (12) and (15), $E\{d_{G(t)}\}$ is represented as:

$$\kappa(G(t)) \leq E\{d_{G(t)}\} = \Lambda W = \lambda \cdot \overline{T}_{link} = \frac{1}{2}\eta_l \cdot \overline{T}_{link}, \quad (16)$$

where $\overline{T}_{link}$ derived in (11) is the function of node target speed v_α and transmission range R. And λ derived in (14) is the function of node density σ, R and v_α. According to (16), Fig. 7 illustrates the relationship among $E\{d_{G(t)}\}$, v_α, and σ for a MANET $G(t)$ with a fixed transmission range $R = 250$ m. As an illustration, for the network with a node density $\sigma = 20/\pi R^2$, when nodes move at target speed $v_\alpha = 20$ m/s, the expected number of neighboring nodes $E\{d_{G(t)}\}$ observed by a specific node at an arbitrary time t is 5. In Fig. 7, we found that the impact of node speed on average node degree $E\{d_{G(t)}\}$ is more significant than the node density σ. This is because the expected new link arrival rate λ rises linearly with the increase of the node density, while the expected link lifetime $\overline{T}_{link}$ decreases exponentially with the growth of node target speed. According to Fig. 7, given a fixed σ, $E\{d_{G(t)}\}$ is generally 4 times larger for nodes moving at the target speed of 2 m/sec than those at the target speed of 20 m/sec. Given (12), (15) and (16), we found the upper bound connectivity of a MANET can be directly obtained from the values of expected link lifetime $\overline{T}_{link}$ and expected link change rate η_l. Hence, these two topology metrics establish a clear relationship among network connectivity, topology dynamics and node mobility in a MANET.

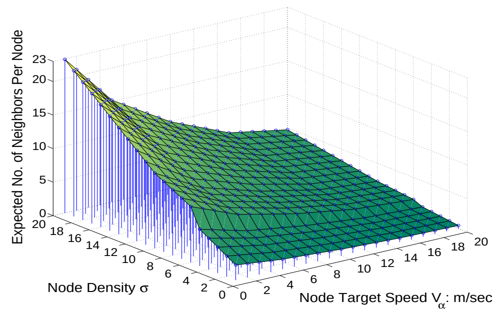

Fig. 7. Expected number of neighbors per node according to different node target speeds v_α and node density σ= number/πR^2, where $R = 250$m.

IV. Conclusions

In this paper, we studied topology dynamics by analyzing MANET link properties under the smooth mobility model because it generates smooth node movements, holds stable node speed and maintains a uniform node distribution. To mimic a realistic moving scenario of MANETs, we provided a relative movement trajectory model, in which the relative velocity of two mobile nodes changes during their link connection. We developed a distance transition probability matrix $\mathbf{P}$, so that we can predict the future link status based on the the present distance between two neighboring nodes and their relative speed. Hence, by using the matrix $\mathbf{P}$, we derived the analytical results of expected link lifetime $\overline{T}_{link}$ and expected link change rate η_l, and further validated them by extensive simulations. Finally, we applied these two topology metrics $\overline{T}_{link}$ and η_l to formulate the upper bound connectivity of a MANET. Our study in this paper can help people on mobility related research issues of MANETs, such as routing protocol design and topology control optimization.

References

[1] M. Zhao and W. Wang, "A novel semi-markov smooth mobility model for mobile ad hoc networks," in *Proc. of IEEE Global Telecommunications Conference (GLOBECOM)*, November 2006.

[2] T. Camp, J. Boleng, and V. Davies, "A survey of mobility models for ad hoc networks research," *Wireless Communication and Mobile Computing (WCMC): Special issue on Mobile Ad Hoc Networking: Research, Trends and Applications*, vol. 2, no. 5, pp. 483–502, 2002.

[3] F. Bai and A. Helmy, "A survey of mobility models in wireless ad hoc networks, to appear on book wireless ad hoc and sensor networks." [Online]. Available: http://nile.usc.edu/˜helmy/Modified-Chapter1-5-30-04.pdf

[4] D. B. Johnson and D. A. Maltz, "Dynamic source routing in ad hoc wireless networks," in *Mobile Computing*. Kluwer Academic Publishers, 1996, vol. 353.

[5] J. Yoon, M. Liu, and B. Noble, "Random waypoint considered harmful," in *Proc. of IEEE INFOCOM*, 2003.

[6] C. Bettstetter, G. Resta, and P. Santi, "The node distribution of the random waypoint mobility model for wireless ad hoc networks," *IEEE Transactions on Mobile Computing*, vol. 2, no. 3, pp. 257–269, 2003.

[7] S. Xu, K. Blackmore, and H. Jones, "Assessment for manets requiring persistent links," in *Proc. of International Workshop on Wireless Traffic Measurements and Modeling WitMeMo'05*, 2005, pp. 39–44.

[8] A. B. McDonald and T. F. Znati, "A moblility-based framework for adaptive clustering in wireless ad hoc networks," *IEEE Journal on Selected Areas in Communications*, vol. 17, no. 8, pp. 1466–1487, August 1999.

[9] A. Papoulis, *Probability, Random Variables,and Stochastic Process*. McGraw-Hill, 1991.

[10] P. Samar and S. B. Wicker, "On the behavior of communication links of node in a multi-hop mobile environment," in *Proc. of ACM MobiHoc*, May 2004.

[11] B. Bollobas, *Modern Graph Theory*. Springer, 1998.